C. R. Physique 14 (2013) 169–184

Contents lists available at SciVerse ScienceDirect

Comptes Rendus Physique

www.sciencedirect.com

Crystal growth / Croissance cristalline

Growth of large size diamond single crystals by plasma assisted chemical vapour deposition: Recent achievements and remaining challenges

Croissance de monocristaux de diamant de grande dimension par dépôt chimique en phase vapeur assisté par plasma : Réalisations récentes et défis à venir

Alexandre Tallaire *, Jocelyn Achard, François Silva, Ovidiu Brinza, Alix Gicquel

Université Paris-13, Sorbonne Paris Cité, Laboratoire des sciences des procédés et des matériaux, CNRS (UPR 3407), 93430 Villetaneuse, France

ARTICLE INFO

Article history:
Available online 18 February 2013

Keywords:
Diamond
Crystal growth
Chemical vapour deposition
Microwave plasma
Defects
Doping

Mots-clés :
Diamant
Croissance cristalline
Dépôt chimique en phase vapeur
Plasma micro-onde
Défauts
Dopage

ABSTRACT

Diamond is a material with outstanding properties making it particularly suited for high added-value applications such as optical windows, power electronics, radiation detection, quantum information, bio-sensing and many others. Tremendous progresses in its synthesis by microwave plasma assisted chemical vapour deposition have allowed obtaining single crystal optical-grade material with thicknesses of up to a few millimetres. However the requirements in terms of size, purity and crystalline quality are getting more and more difficult to achieve with respect to the forecasted applications, thus pushing the synthesis method to its scientific and technological limits. In this paper, after a short description of the operating principles of the growth technique, the challenges of increasing crystal dimensions both laterally and vertically, decreasing and controlling point and extended defects as well as modulating crystal conductivity by an efficient doping will be detailed before offering some insights into ways to overcome them.

RÉSUMÉ

Le diamant est un matériau aux propriétés hors du commun permettant d'envisager un grand nombre d'applications, parmi lesquelles des fenêtres optiques, des dispositifs d'électronique de puissance ou d'information quantique, des détecteurs de radiation ou de substances biologiques. Les énormes progrès de la technique de synthèse par dépôt chimique en phase vapeur assisté par plasma micro-onde ont permis la réalisation de monocristaux de qualité optique jusqu'à plusieurs millimètres d'épaisseur et présentant une bonne transparence. Néanmoins, les exigences en termes de dimensions, de pureté et qualité cristalline sont de plus en plus élevées pour les applications visées, et la croissance se heurte alors à un certain nombre de verrous technologiques ou scientifiques. Dans ce papier, après une rapide description des principes de la technique de croissance, les problèmes de l'augmentation des dimensions verticales et latérales des cristaux, du contrôle des défauts ponctuels et étendus ainsi que de la modulation de la conductivité par l'ajout d'impuretés dopantes seront abordés et des solutions possibles seront alors proposées.

* Corresponding author.
E-mail address: alexandre.tallaire@lspm.cnrs.fr (A. Tallaire).

1631-0705/$ – see front matter
http://dx.doi.org/10.1016/j.crhy.2012.10.008

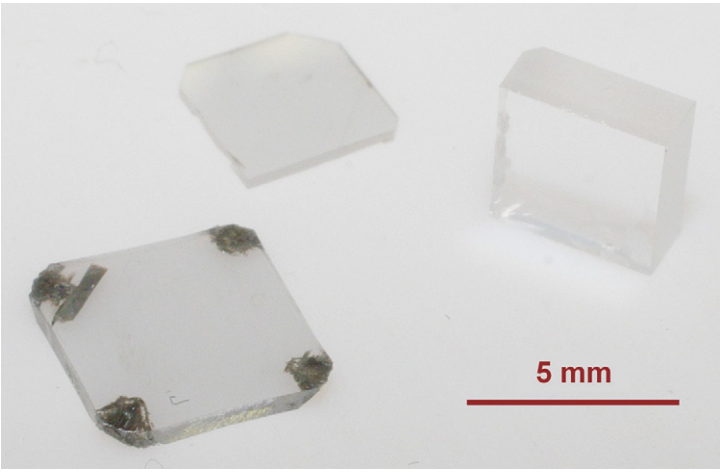

Fig. 1. High-purity freestanding CVD diamond single crystals synthesized at LSPM-CNRS.
Fig. 1. Monocristaux de diamant auto-supportés de haute-pureté synthétisés au LSPM-CNRS.

1. Introduction

Single crystal diamond is well-known as an attractive gem stone due to its eye-catching sparkle or fancy colouration. However the scientific interest that has surrounded this material for the past decades is altogether different. Indeed single crystal diamond possesses several outstanding properties such as an unrivalled thermal conductivity ($> 2000\ \mathrm{W\,cm^{-2}\,K^{-1}}$), carrier mobilities that can reach a few thousands of $\mathrm{cm^2\,V^{-1}\,s^{-1}}$, a high breakdown voltage and a large bandgap (5.5 eV) together with exceptional hardness and resistance to harsh environments.

Natural diamond being an unreliable source of material, technical applications mostly rely on synthetic diamonds that are produced by the High Pressure High Temperature technique (HPHT) [1]. However incorporated impurities: essentially nitrogen but also boron, cobalt or nickel [2] originating from the metal catalyst solvents are commonly found at levels of a few parts per million (ppm) [3]. HPHT diamonds are thus essentially classified as type-*Ib* crystals (yellow-coloured). Excluding these impurities in order to produce uncoloured type-*IIa* crystals [4,5] is possible at the expense of a considerable reduction in the optimal window of growth conditions and at much lower growth rates making the process scaling up particularly difficult. Generally speaking, the accurate control of point defects in HPHT crystals is not straightforward. Increasing attention has thus focused on a low pressure technique, Plasma Assisted Chemical Vapour Deposition (PACVD) that holds great promise to grow "electronic-grade" single crystal films with tailored properties.

The past two decades have witnessed significant breakthroughs in CVD diamond synthesis. While the technique was initially limited to the deposition of thin films at growth rates of the order of 1 μm/h or below, with a relatively poor quality or with a polycrystalline structure, tremendous improvements of the process have later allowed reaching much higher growth rates and crystal morphologies free of unepitaxial defects [6–10]. Millimetre-size gem-quality diamond crystals were demonstrated in the mid 2000s [11,12]. Fig. 1 shows diamond films with thicknesses of up to 2 mm exhibiting high purity with a nitrogen content typically below 1 ppb (part per billion) synthesized in our group at LSPM [13]. Only very recently have type-*IIa* CVD diamond single crystal plates (with an area of a few $\mathrm{mm^2}$) become commercially available from one supplier [14]. As a basic material, they have spurred renewed interest in a wide range of high technology applications.

Among them, power electronics could take advantage of diamond's high breakdown field for fabricating devices operating at high voltage and current [15], efficiently replacing the current silicon technologies that have reached their physical limits [16]. Using diamond films for thermal management is also a possible way to improve the performance of electronic devices such as nitride transistors [17,18]. The control of nitrogen-related defects in ultra-high purity diamond is currently at the spotlight due to their unique spin coherence properties that could open the way to room temperature quantum computing [19,20]. Optical components based on low-birefringent diamond single crystals are also particularly interesting for power-laser windows or for Raman lasers [21,22]. Finally radiation-hard or solar-blind detectors for UV light or high-energy particles with unrivalled characteristics could be designed for radiotherapy [23], astrophysics or high-energy physics [24]. These are only a few of the high added-value applications that could be developed with diamond.

However, the availability of synthetic diamond crystals with the relevant properties suitable for these applications still remains relatively limited as the requirements in terms of quality, purity and dimensions are getting more and more stringent. The challenges that arise in terms of material are of several kinds: (i) the crystal dimensions should be increased both laterally and vertically to permit device processing and increase the available active area to a few $\mathrm{cm^2}$; (ii) a perfect control over point and extended defects should be reached; dislocation densities reduced, impurities and vacancies limited and isotopic purity controlled; (iii) finally efficient doping of the crystal with both *p* and *n*-type impurities should be achieved in a wide range of concentrations and spatially controlled within the crystal structure.

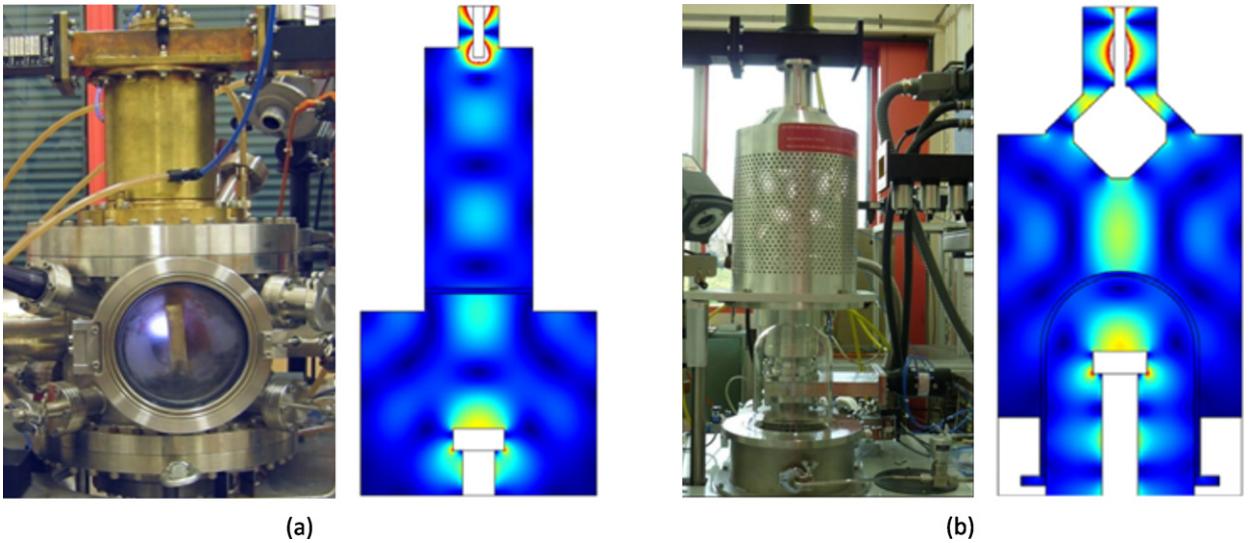

Fig. 2. PACVD reactors and their electric field distribution. Light red colour indicates higher electric field. (a) Home-made metallic-chamber reactor; (b) bell-jar reactor co-developed between LSPM and Plassys company, showed opened on the picture.

Fig. 2. Images et distribution du champ électrique modélisé dans les réacteurs PACVD. La couleur rouge indique un champ électrique plus élevé. (a) Réacteur à chambre métallique, (b) réacteur de type « bell-jar » co-développé entre le LSPM et l'entreprise Plassys, montré avec la cage relevée sur l'image.

At LSPM we have devoted substantial efforts in trying to tackle those issues in the past several years. In this paper, after a short description of the operating principles of the PACVD technique, the challenges of increasing the crystal dimensions, decreasing and controlling defects as well as mastering *p*-type doping will be detailed before offering some insights into ways to overcome them.

2. The PACVD process

In the PACVD process, diamond is synthesized using activated hydrogen-rich H_2/CH_4 gas mixtures under non-equilibrium conditions where graphite is supposedly the stable form of carbon. Methyl radicals (CH_3), produced from the dissociation of methane, are widely accepted as being the main hydrocarbon precursor species [25]. H_2 also dissociates into atomic hydrogen within the plasma, which plays a key role in kinetically stabilizing the diamond phase as well as etching non-diamond phases (sp^2 carbon). In fact, growing diamond films with high quality and at high growth rates mostly relies on the ability to produce a large amount of atomic hydrogen in the vicinity of the growing surface [26–28]. Despite the simple gas mixture, the number of reactions and chemical species involved can be extremely complex and extensive works – both modelling and experimental studies – have dealt with determining species densities and distribution within the plasma, and their transport and consumption at the surface depending on the input parameters (pressure, temperature, power density etc.) [29,30]. These works have helped highlighting the key parameters for diamond growth.

The most common way to transfer energy to the gas phase so as to ignite plasma is through microwave (MW) radiation. Typical operating pressures range from low (a few tens of mbar) to moderate pressure (a few hundreds of mbar) with coupled MW powers of 600 to 6000 W. The microwave power density (MWPD) which represents the ratio between the injected power to the size of the plasma ball has a strong influence on the growth process. High MWPD (i.e. high pressure and MW power) promotes gas phase thermal dissociation thus enhancing growth rates and improving crystal quality. Processes operating at high-power where temperatures in the plasma core reach up to 3500 K are thus preferred to grow thick diamond films (see Section 3.1) [13,31].

There exist several reactor technologies for growing diamond; most of them use resonant electromagnetic cavities suitable to produce plasma at a relatively high pressure near the substrate with a typical size of the order of 2 to 3 inches when typical 2.45 GHz MW radiation is used [32–34]. At lower MW frequency (such as 915 MHz) the size of the plasma ball and the deposited area can be increased up to 6 inches. A proper design of the resonant cavity is particularly crucial in the high power conditions required for diamond growth so that most of the injected MW power is used to heat the gas phase and is not lost in heating-up the wave-guide or the reactor chamber walls. The plasma should also be contained in a low pressure chamber that can be the MW cavity itself in the case of metallic-type reactors (Fig. 2a) or a quartz jar in the case of "bell-jar" reactors (Fig. 2b). Quartz jars present the advantage of being easily exchangeable for cleaning and avoiding cross-contaminations with doping species but can also lead to Si incorporation into the films and are more difficult to cool-down. Electromagnetic modelling of PACVD reactors has been carried out at LSPM and has allowed developing the efficient systems presented in Fig. 2.

Epitaxial diamond growth by the PACVD process also suffers from the limited availability of substrates that can be used. Although intense research efforts have been devoted to try to improve the quality of heteroepitaxial diamond films, there is

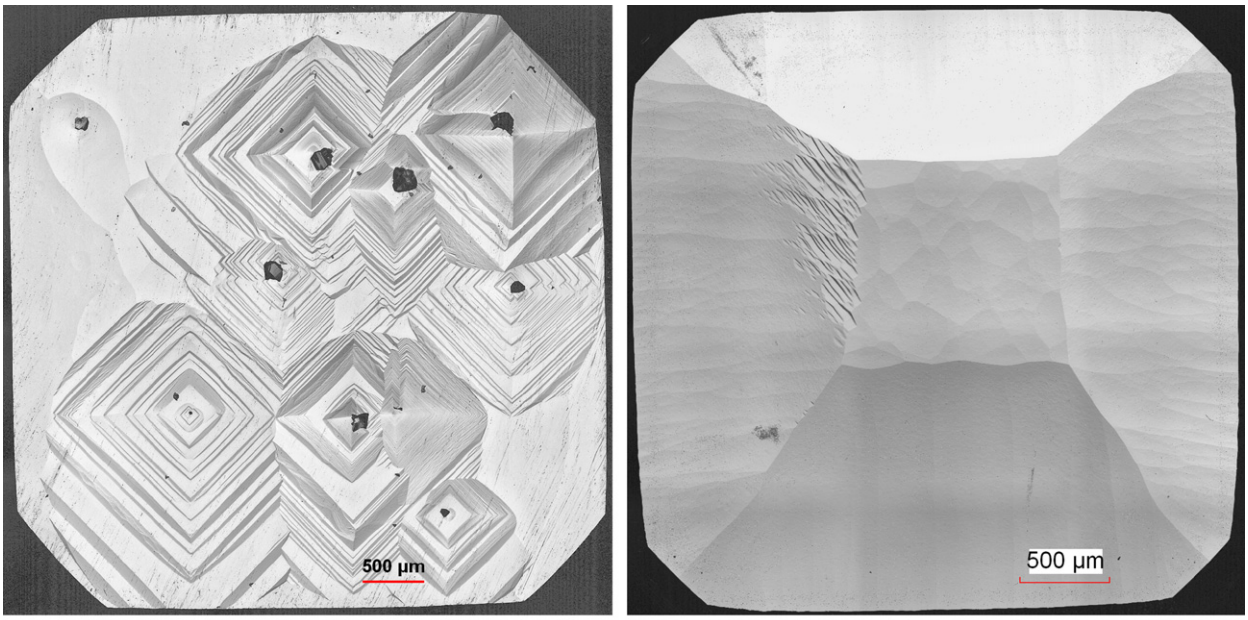

Fig. 3. Effect of growth temperature. Confocal laser microscopy images of 160 µm thick CVD films grown at (a) 920 °C, 7 µm/h, (b) 870 °C, 6 µm/h.

Fig. 3. Effet de la température de croissance. Images en microscopie confocale laser de films CVD de 160 µm d'épaisseur élaborés à (a) 920 °C, 7 µm/h, (b) 870 °C, 6 µm/h.

still a lack of an appropriate non-diamond substrate. Fairly good results have been reported using iridium [35,36] but defect densities are still too high for most applications. Consequently, single crystal growth must be carried out homoepitaxially on a diamond seed. Since large area type-*IIa* seeds are not easily accessible or at a prohibitive cost, the most widespread substrates are type-*Ib* HPHT diamonds commercialized as cutting tools, having an area of a few mm^2 and preferably (100)-oriented to avoid twinning [37]. Although large dimensions cannot be easily achieved, several tens of seeds can be treated in a single run [38].

3. The growth of single crystal diamond with large dimensions

3.1. Increasing growth rates

If thick diamond single crystals are to be produced using a viable process, high deposition rates should be reached so that growth is carried out within a reasonable time. This is further complicated by the difficulty in maintaining stable growth conditions (temperature, cleanliness of the chamber, ...) during extensive periods of time. There exist several tuning parameters for the crystal grower to increase growth rates.

One possibility is to raise deposition temperatures in order to increase the number of surface active sites and to promote species diffusion and surface reactions [39]. In fact it is well-known, especially for polycrystalline films that growth rates increase following an Arrhenius law, exhibiting a maximum at around 1000 °C depending on pressure after which species desorption and surface etching governs [40,41]. However going to so high a temperature under high purity conditions plagues the surface morphologies for single crystal diamond. Above 900 °C, we observe a roughening of the crystal surface due to the formation of typical pyramidal defects (Fig. 3a, 920 °C, 7 µm/h) while at reasonably lower temperature the surface remains smooth (Fig. 3b, 870 °C, 6 µm/h). At high temperature twinning is promoted on existing defects such as screw dislocations emerging at the surface. Moreover a favourable ratio of growth rates in ⟨100⟩ and ⟨111⟩ directions (defining the α parameter) ensures that once formed twins will survive and overgrow [42]. Adding N_2 usually prevents the formation of twins on (100) surfaces allowing extending the maximum deposition temperature to a higher value [43,44] but at the expense of crystal purity. The acceptable temperature range is relatively narrow and there is only little room for growth rate improvement using this parameter.

The addition of N_2 even at rates as low as a few ppm in the gas phase strongly boosts up crystal growth rates on ⟨100⟩ orientations by catalytic effect [45,46]. Fig. 4 shows that 10 ppm of N_2 improves growth rates by more than a factor of 2 enabling the growth of uncoloured "optical-grade" freestanding CVD diamond films. Considering the improvement in crystal morphologies previously stated it is not surprising that most studies reporting the synthesis of millimetre-thick crystals were usually performed with addition of several hundreds of ppm of N_2 [8,12,43]. However nitrogen incorporates

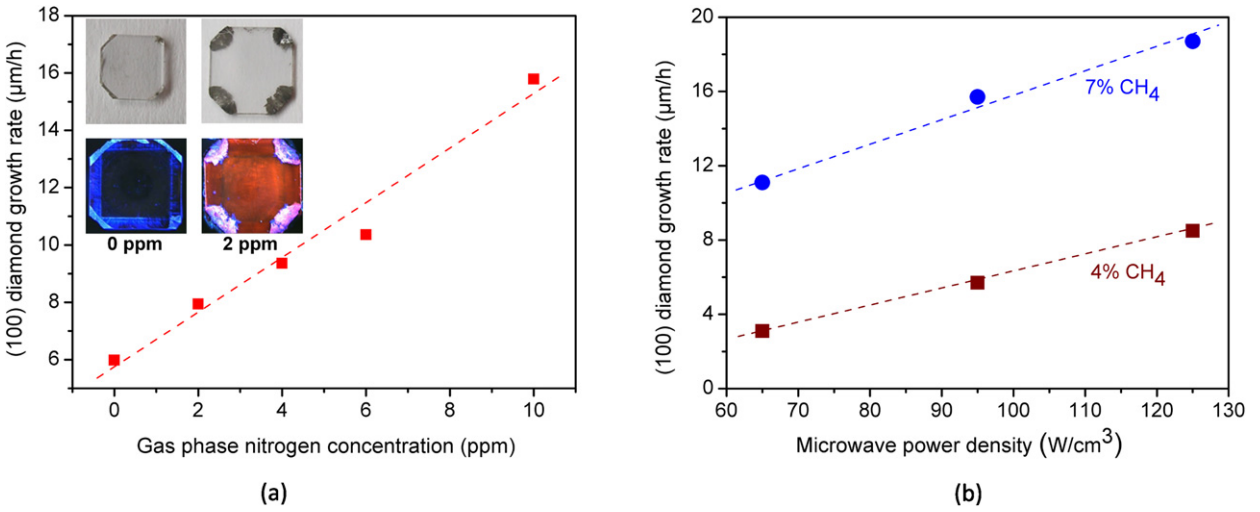

Fig. 4. (a) Diamond growth rate as a function of nitrogen addition in the gas phase (MWPD = 95 W/cm^3). Optical and PL images obtained under UV light for an undoped freestanding CVD diamond crystal and a 2 ppm N_2 doped. (b) Evolution of the growth rate as a function of microwave power density at a constant surface temperature (850 °C) and for different methane concentrations.

Fig. 4. (a) Vitesse de croissance en fonction de la concentration en azote dans la phase gazeuse (MWPD = 95 W/cm^3). Image optique et de PL obtenue sous UV pour un film non dopé et dopé avec 2 ppm. (b) Évolution de la vitesse de croissance en fonction de la densité de puissance micro-onde à une température de surface constante (850 °C) et pour différentes concentrations en méthane.

and drastically deteriorates the electronic properties. Introducing a small amount of impurities can only be considered as a viable way to improve growth rates for optical and thermal applications of diamond.

When the (001) top surface is polished with an off-angle of 2 to 20°, growth rates are enhanced due to the presence of a higher density of growth steps [47]. On vicinal faces the development of unepitaxial defects is suppressed leading to smooth surfaces [7]. However the uptake of impurities is also higher [48] and, after some time, because the surface tends to become exactly oriented again the growth rate enhancement stops. To some extent the use of misoriented substrates is a possible but very limited way to grow thicker films.

As previously stated, gas phase dissociation plays a key role in producing precursor species for diamond growth, especially hydrogen. Under the moderate pressures used in the reactor, dissociation is mainly thermal, occurring in the hot plasma core. Improving the production of atomic hydrogen thus relies on the ability to use higher MWPD (both MW power and pressure) to obtain a hot and confined plasma. Fig. 4b shows growth rates as a function of power densities obtained in a metallic-type reactor, illustrating that power densities above 70 W/cm^3 are a requisite for growing thick diamond crystals in such reactors [49]. The upper limit of this parameter is mostly technological. Coupling high power densities generates huge heat fluxes and can overheat the reactor chamber walls or the growing crystal. Etching of the chamber walls or windows can also lead to silicon contamination. To work around this issue, the use of pulsed discharges has been proposed allowing having very high peak powers but with moderate average powers thus somehow decorrelating species production and thermal effects [50–52].

An alternative to an increase of the MWPD is to improve thermal confinement of the plasma through the addition of a gas having a lower thermal conductivity than H_2 [53,54]. By adding up to 40% argon to the gas mixture, we have measured an increase of 500 K of the gas temperature and correlatively an improvement of the growth rates by a factor of 2 (Fig. 5a) without any noticeable effect on surface morphologies [55]. This is consistent with an increase in the production of atomic hydrogen observed by modelling (Fig. 5b).

Finally growth rates roughly scale as the square root of the CH_4 concentration in the gas phase. At low power density and particularly for polycrystalline diamond, above a few % of methane, growth rates dramatically drop [56]. Surface morphology changes due to the appearance of secondary nucleation and crystalline quality is lower than at low CH_4/H_2 ratio [57]. At high power densities though, the amount of atomic hydrogen produced in the plasma is high enough to counterbalance the increase in carbon-containing species, preventing formation of defects or sp^2 phases. In that case the main limiting factor is the production of soot in the plasma that accumulates on the reactor's quartz windows, absorbing the injected MW power and imposing the growth run to be aborted. In our reactors and under typical conditions this occurs for CH_4 concentrations of the order of 8–10%. The appearance of soot can sometimes be delayed by the addition of other gases such as oxygen [58] or by changing the gas flow and hydrodynamics inside the chamber but further work is required to fully understand their mechanisms of production.

It can be seen that there exist several possibilities to increase diamond growth rates, the most efficient being the joint increase of microwave power density and methane concentration in the gas phase on the condition that reactors are properly designed to deal with elevated heat fluxes and possible formation of soot. In that case, growth rates of the order of a few tens of µm/h (typically 20 µm/h) can be reached under high purity conditions and in a reproducible way.

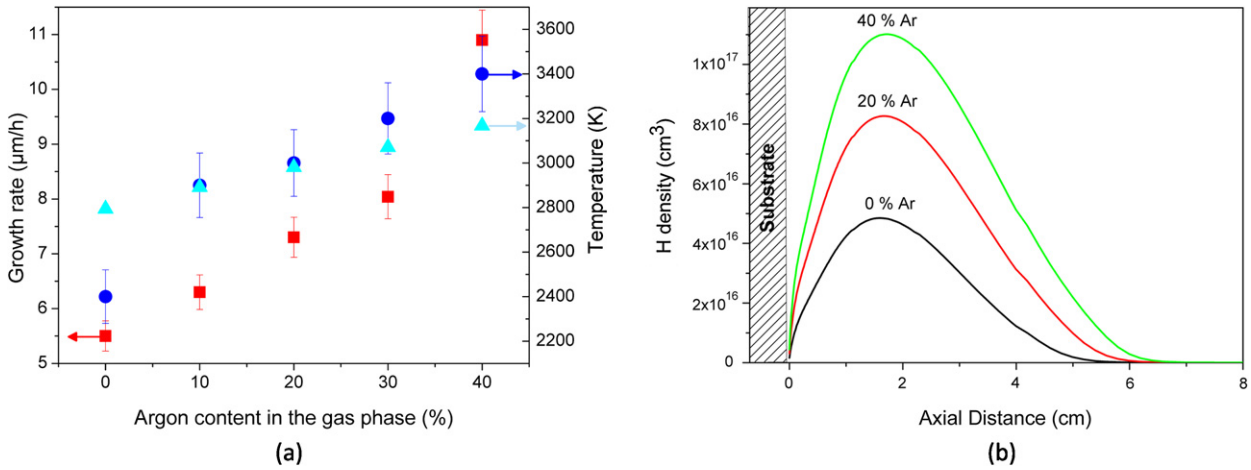

Fig. 5. (a) Effect of argon addition on diamond growth rates and on gas temperatures calculated from the optical emission of C_2 Swan system (blue circles) and calculated using a 1D plasma model (light blue triangles) (MWPD = 95 W/cm^3). (b) Modelling of the effect of argon on atomic hydrogen density in the plasma as a function of the distance from the substrate.

Fig. 5. (a) Effet de l'ajout d'argon sur les vitesses de croissance et sur les températures de gaz calculées à partir de l'émission optique du C_2 du système Swan (ronds bleus) et calculés au moyen d'un modèle plasma 1D (triangles bleus clairs) (MWPD = 95 W/cm^3). (b) Modélisation de l'effet de l'argon sur la production d'hydrogène atomique dans le plasma en fonction de la distance au substrat.

3.2. Towards thicker crystals

The interest in thick crystals does not necessarily stem from their being more attractive as gems but rather because larger dimensions unlock the possibility to process them into plates with the desired crystallographic orientation. For example, (111) plates could be sliced from a large CVD stone or several plates could be prepared by cutting the crystal parallel to the growth direction which will affect dislocation networks (see Section 4.2). Growing millimetre-thick high-purity crystals relies on achieving fast growth rate, but it is also essential to be able to control crystal morphologies all along the growth process.

Growth conditions must be adapted in order to prevent the formation of undesirable faces and to ensure that as much as possible only a large (001) top face, free of any defects, develops. Knowing the growth rates of different crystal faces, a geometrical model has been developed at LSPM to predict the evolution of the crystal shape with time [59,60,42]. Figs. 6a and 6b show the predicted and real morphology of a 500 µm thick CVD diamond film grown on a cubic shape substrate having {100} top and lateral faces. During growth, {110} faces appear at the edges of the crystal, {113} and sometimes {111} faces are also formed at the corners. {113} faces usually have the lowest growth rate and they should remain for infinite growth times (steady-state shape) [61]. Depending on the growth conditions chosen (temperature, methane concentration, addition of O_2 for example) the growth rate of these faces relatively to each other will change (Figs. 6c and 6d). Therefore it is possible to slightly tune the transient or final shape of the crystal by adapting the growth conditions, although the degree of freedom is relatively limited due to a narrow optimal window of deposition. For example, large {110} faces induce stress in the crystal, sometimes causing it to break apart [62]. Conditions inhibiting the appearance of {110} faces, i.e. higher temperature or lower CH_4 concentration, should thus be preferred.

Besides the evolution of the crystal shape, another limiting factor to the growth of very thick crystals is the formation of unepitaxial features particularly at the corners of the crystal on {111} and {110} faces. When thicknesses higher than a few hundred micrometres are reached, these defects become prominent and start encroaching on the top (001) surface (Figs. 7a and 7b), possibly causing the corners to fracture. Growth conditions can be chosen to delay the appearance of such defects but most of the time the growth needs to be interrupted. Resuming growth requires that edges are laser cut and the top surface to be re-polished so as to obtain thick crystals such as that shown in Figs. 7c and 7d. This further complicates the synthesis of thick plates all the more as growth interruptions generate new defects and preferential incorporation of impurities at the interface [63].

The growth of millimetre-thick high-purity crystals is thus not straightforward and substantial efforts must be dedicated to control the crystal shape and stress as well as limit twinning at the edges without N_2 addition.

3.3. Towards large area single crystals

When it deals with increasing the crystal dimensions, the most challenging task is definitely that of obtaining large area crystals that could be used as wafers for electronics. Because growth is carried out homoepitaxially, the final area is intrinsically limited by that of the diamond substrate which is rarely above a few tens of mm^2.

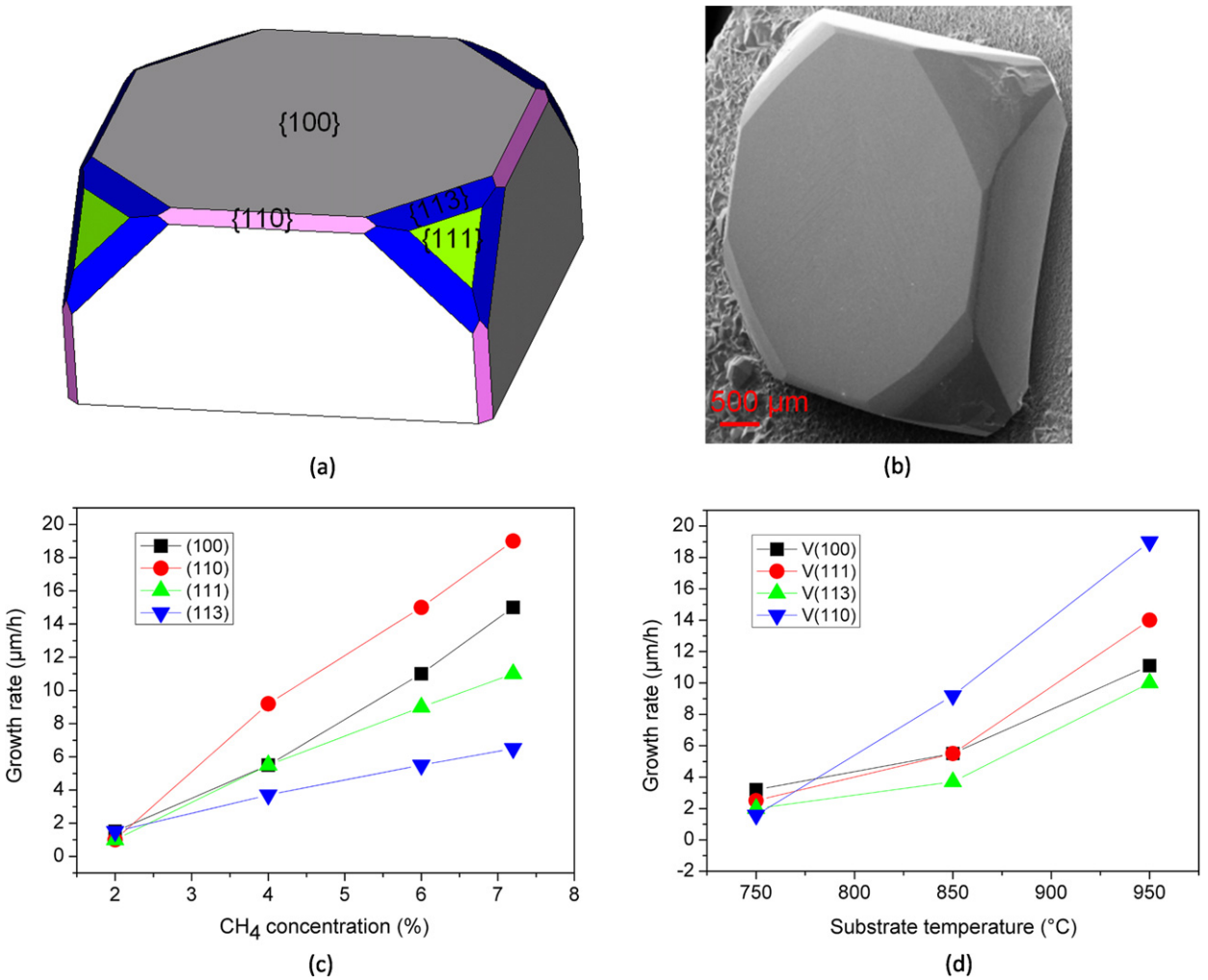

Fig. 6. (a) Predicted morphology of a 500 µm thick CVD film grown on a (100) HPHT substrate; (100) faces are in white, (110) faces in pink, (113) faces in blue, (111) faces in green. (b) Scanning electron microscope image of a typical CVD film on its HPHT substrate; (c) and (d) evolution of the growth rates of different crystal planes as a function of CH_4 concentration and surface temperature.

Fig. 6. (a) Morphologie prédite pour un film de 500 µm déposé sur un substrat orienté (100) ; faces (100) en blanc, (110) en rose, (113) en bleu, (111) en vert. (b) Image en microscopie électronique à balayage d'un film typique sur un substrat HPHT ; (c) et (d) évolution des vitesses de croissance des différents plans cristallins en fonction de la concentration en méthane et de la température de surface.

Since growth also occurs on the lateral faces of the initial diamond seed, enlargement is usually observed for a crystal having both top and lateral sides {100}-oriented [64]. For example if the initial HPHT substrate is 3.5×3.5 mm^2, the final area obtained for a deposited thickness of 1700 µm as illustrated in Fig. 7c will be more than 6×6 mm^2, after the central square has gone through 45° "rotation". Geometrical modelling has shown that when this rotation is completed, the lateral sides are {110}-oriented and the top surface area will decrease again due to the development of {113} faces at the edges of the crystal that have the slowest growth rate [64]. Note that on Fig. 7c these faces are prone to twinning again as unepitaxial defects are seen around the edges. This enlargement is therefore intrinsically limited to a few tens of mm^2 and it requires that relatively thick films of a few hundreds to a few thousands of micrometres are grown.

Other authors have proposed alternative growths on the top and lateral sides to increase the diamond area [65]. The crystal is grown vertically for several millimetres at high rate using N_2 impurities. One of the lateral sides is then laser-cut, polished and exposed again to the plasma allowing enlarging the crystal up to 10×10 mm^2. The resulting crystal quality however remains poor due to N incorporation and twinning, and the processing steps are time-consuming which makes this technique unsuitable in the present form.

Among all enlargement techniques, the growth of mosaic crystals which has been proposed several years ago [66–68] has attracted the most attention in the last few years [69]. It consists of close-packing several small single crystal substrates

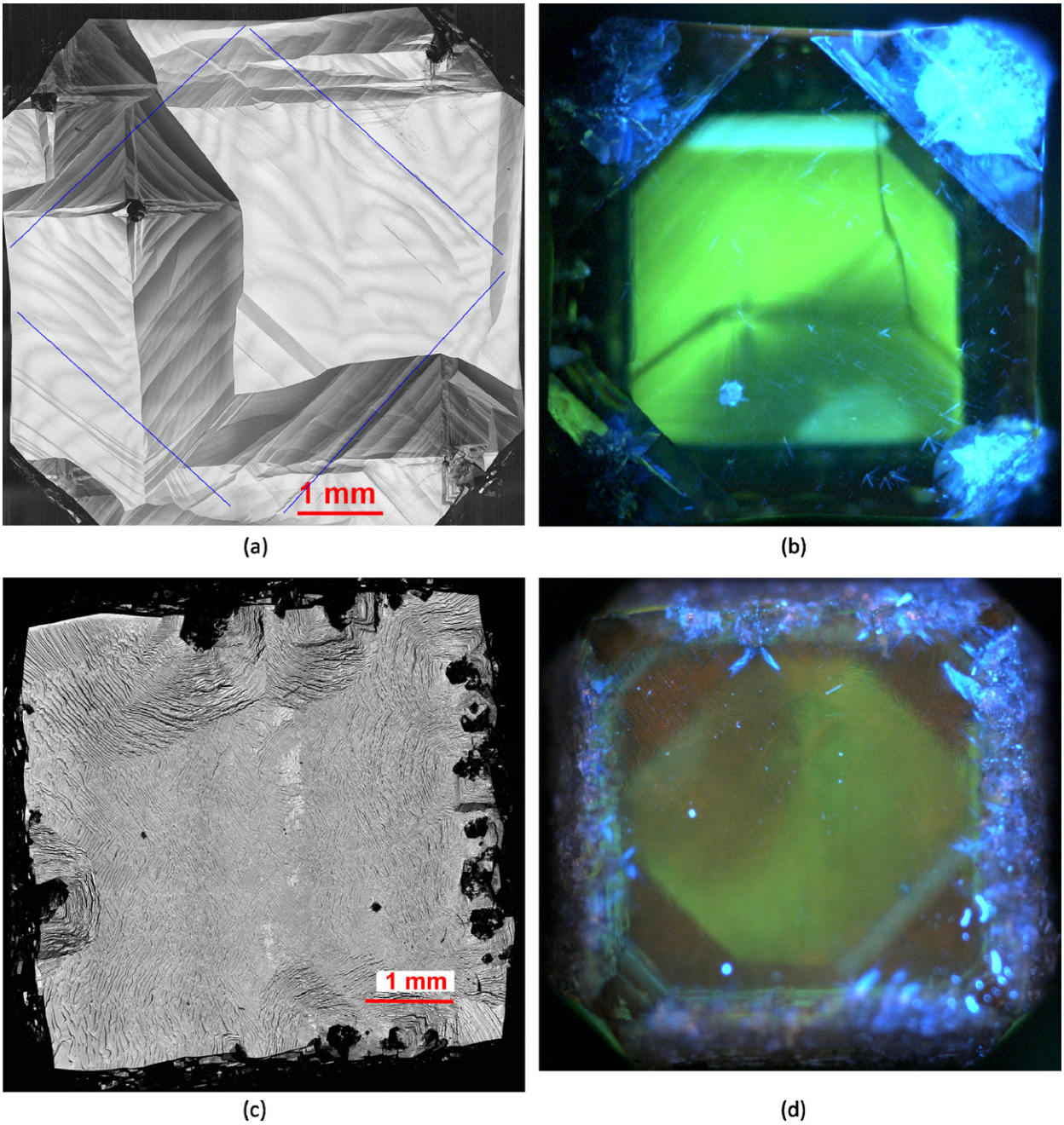

Fig. 7. 900 µm thick CVD diamond film (a) showing twinning and defect nucleation from the corners inducing cracks and stress visible on the UV PL image (b). The crystal was laser-cut along the blue lines and growth resumed to reach a total thickness of 1700 µm (c). Twinning occurred again at the edges of the crystal. Note that on the PL image (d) the green square corresponding to the HPHT substrate is 45° rotated.

Fig. 7. Film CVD de 900 µm (a) présentant du maclage et des défauts au niveau des coins qui induisent de la contrainte et de la fissuration visible sur l'image de PL UV (b). Le cristal a été découpé par laser le long des lignes bleus et la croissance reprise pour obtenir une épaisseur totale de 1700 µm (c). Le maclage apparaît à nouveau sur les arêtes du cristal. On notera que sur l'image de PL (d) le carré vert correspondant au substrat HPHT est tourné de 45°.

so that the grown layer on top of the assembly merge and cover the entire area. This technique requires a very critical preparation and alignment of individual substrates since any misorientation, height difference or gap between adjacent substrates will induce stress in the final crystal leading either to cracking or twinning at the interconnection. Fig. 8a shows an assembly of 7 substrates onto which an 800 µm-thick CVD film was grown. The junctions between substrates show defects and stress (Fig. 8b), but a one-piece CVD layer was successfully obtained. On one occasion excellent interconnections were observed without any visible defects and with minimal enlargement and shift of the diamond Raman peak (Fig. 8c). By assembling CVD layers originating from the same substrate and obtained by lift-off [69,70] – so-called "cloned layers" –

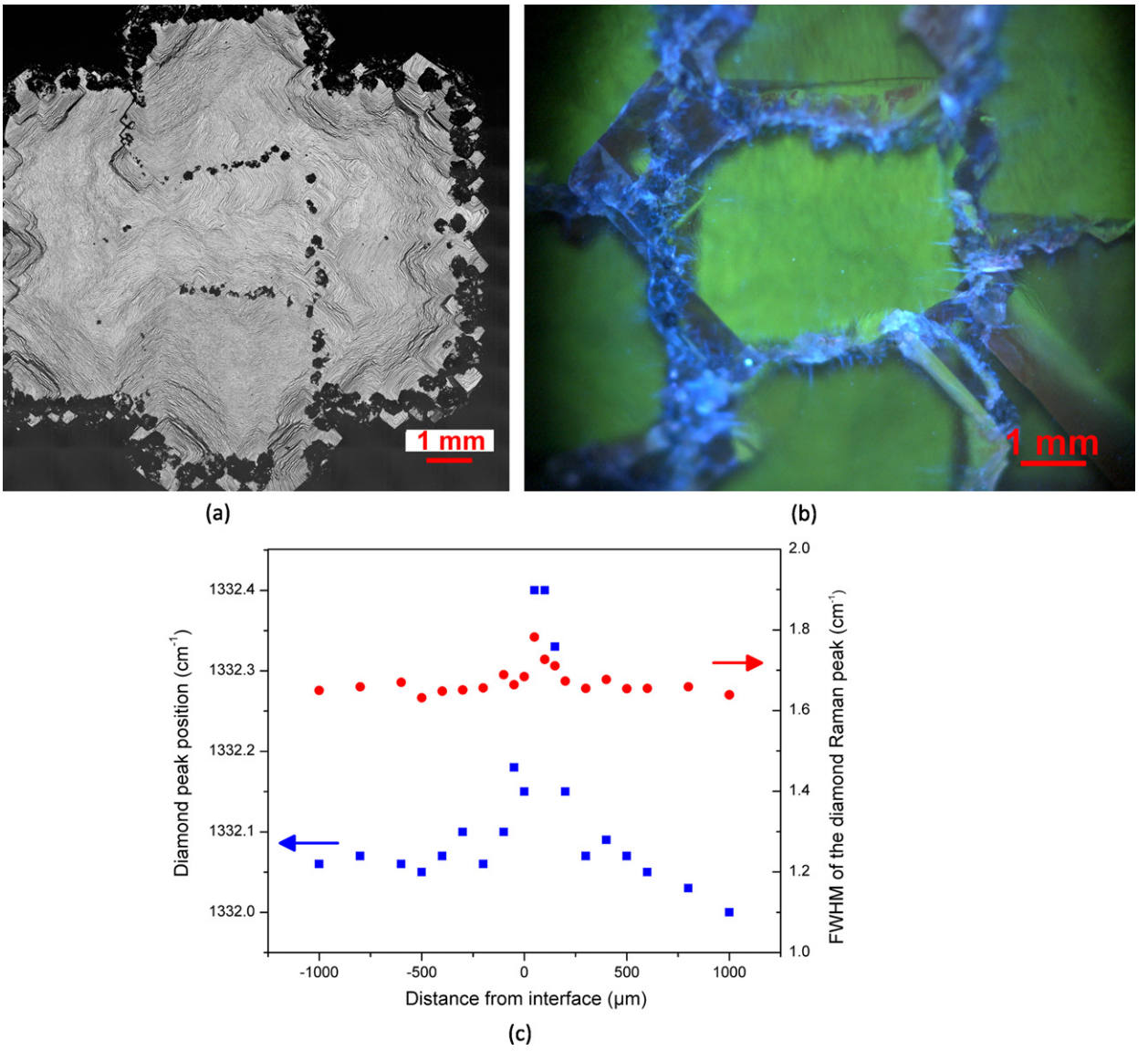

Fig. 8. (a) Image of a mosaic layer grown onto 7 individual HPHT diamond substrates (Collab. IPHC-CNRS and Colorado University). (b) UV PL image at the centre of the mosaic showing the presence of stress and cracks at the interconnection (blue colouration). (c) Raman analysis across a boundary on another sample showing a minimal shift and enlargement of the diamond peak and indicating that crystal quality remained high.

Fig. 8. (a) Image d'un film mosaïque déposé sur 7 substrats individuels (Collab. IPHC-CNRS et Université du Colorado). (b) Image PL sous UV au centre de la mosaïque montrant la présence de contraintes et de fissures (coloration bleue). (c) Analyse Raman au passage d'une interconnection effectuée sur un autre échantillon et montrant un déplacement et un élargissement réduits du pic, indiquant que la qualité cristalline reste élevée.

some authors have obtained one-inch single crystal plates with fairly good properties. Obtaining high quality 2 inch wafers remains the most challenging and still unachieved objective.

4. The control of purity and defects in diamond

4.1. Point defects

The control of point defects in CVD diamond is essential if one wants to achieve device-grade single crystals. Since diamond has a very dense lattice structure composed of tetrahedrally coordinated carbon atoms the incorporation of foreign elements into the crystal is usually relatively difficult. However several impurities have been identified. An exhaustive list of optically active point defects can be found in Ref. [71]. This paper does not intend to review all point defects in diamond but rather to give a short overview of the most common impurities in CVD films and their implication on the growth technique and on possible applications.

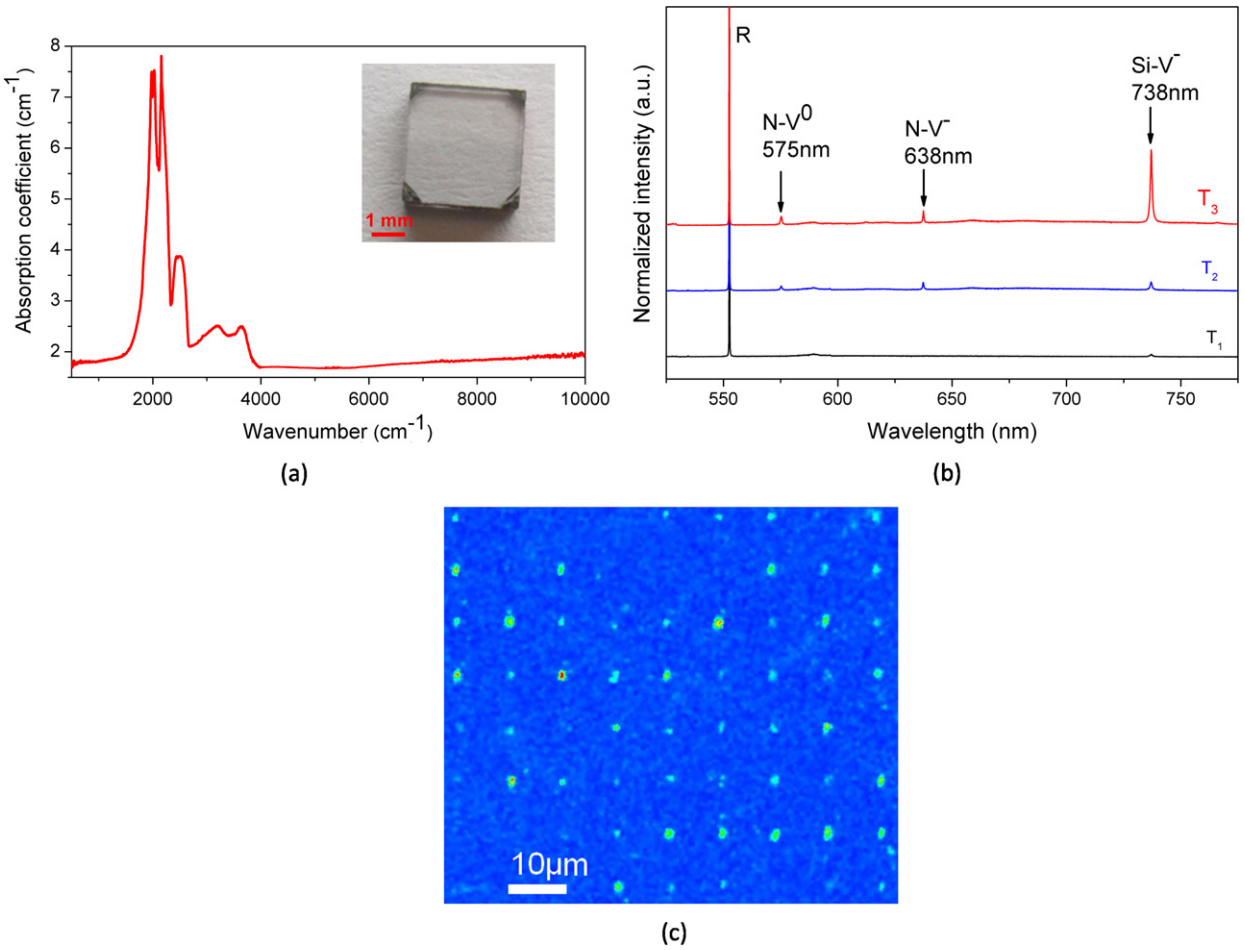

Fig. 9. Point defects in diamond. (a) FTIR spectra of a high-quality CVD crystal showing the intrinsic 2-phonon absorption bands and no detectable impurity; (b) PL spectra of single crystals grown at various temperatures with $T_1 > T_2 > T_3$ showing different luminescent defects (R is the diamond Raman peak); (c) Luminescent emission from an array of NV centres implanted through a mask and observed by confocal microscopy (Collab. ENS-Cachan, Thalès R&T and Rubion Bochum).

Fig. 9. Défauts ponctuels dans le diamant. (a) Spectre FTIR d'un cristal CVD de haute qualité montrant uniquement l'absorption intrinseque à 2 phonons. (b) Spectre de PL de monocristaux synthétisés à différentes températures avec $T_1 > T_2 > T_3$ et montrant des défauts luminescents (R est le pic Raman du diamant) ; (c) Luminescence d'un réseau de centres NV implantés au travers d'un masque et observés en microscopie confocale [80] (Collab. ENS-Cachan, Thalès R&T et Rubion Bochum).

The presence of vacancies in diamond can be enhanced by electron or neutron irradiation giving rise to the well-known GR1 centre having a zero phonon line (ZPL) doublet at 751 and 754 nm which is directly proportional to the irradiation dose. Vacancy clusters are possible candidates for the brown colouration of diamond and have been measured by positron annihilation spectroscopy [72]. Vacancies are mobile at temperatures above 600 °C and can be involved in a number of other defects.

Since diamond films are grown in hydrogen-rich environment, it is not surprising that varying amounts of H-related point defects are detected. The main indication of the presence of H is an absorption band at 3107 cm^{-1} [73] related to the stretching mode vibration of C–H bonds. The negatively charged V–H defect has also been identified in CVD diamond by Glover et al. using Electron Paramagnetic Resonance (EPR) spectroscopy [74]. Hydrogen is believed to passivate boron acceptors [75] probably due to the formation of BH complexes and has recently been pointed out as possibly quenching the emission of NV centres [76]. In high crystalline quality CVD diamond the presence of hydrogen can be relatively limited and even undetectable using Fourier Transform Infrared (FTIR) spectroscopy (Fig. 9a).

Nitrogen impurities are very frequent as they can originate from the feed gas, from leaks in the CVD reactor or desorption of the reactor walls. Due to the low pressure growth conditions, aggregated forms of nitrogen common in both HPHT and natural diamonds are not normally found in untreated CVD films. Isolated substitutional nitrogen atoms (N_s) which concentration can be precisely measured by EPR [77] are fairly common though. When nitrogen is associated to vacancies, other defects are formed such as NV centres that show a luminescence with a ZPL at 575 and 637 nm for the neutral and negatively charged forms respectively (Fig. 9b). Finally other defects are sometimes found but with a lower concentration

such as NVH, also measurable by EPR. When growing under appropriate conditions, using leak tight reactors and purified gases, ultra-high purity diamond crystals can be synthesized with nitrogen contents of the order of a few ppb or even a few ppt (parts per trillion) only, due to the relatively low incorporation efficiency of nitrogen (around 10^{-4}) [78]. The growth conditions in particular the surface temperature also strongly affect the uptake of nitrogen in the films (Fig. 9b).

Among all nitrogen-related defects NV centres have attracted the most attention in the past 10 years due to their ability to behave as stable single photon sources with long coherence time at room temperature. The electron spin of the defect can be polarized in its ground state by optical pumping, manipulated through the use of microwave fields and finally the radiative signal emitted can be read out using confocal microscopy. This defect holds great promise for future quantum computing applications if arrays of NV centres are engineered. When nitrogen implantation is followed by electron irradiation and thermal annealing to generate and diffuse vacancies, NV defects can be produced quite efficiently [79]. Networks of NVs can be obtained either by implantation through a mask (Fig. 9c) [80] or through a nanoaperture made on an AFM tip [81]. However the coherence time of such artificially produced defects is usually quite lower than that of grown-in defects and their accurate localization is plagued by ion channelling and straggling problems. Decoherence of NV centres is strongly influenced by their surrounding neighbours such as defects induced by implantation, surface states [82], or paramagnetic atoms (N_s or C^{13}). Thanks to the ability of synthesizing diamond under a controlled environment the PACVD technique could potentially allow engineering embedded NV centres with unequalled properties. For example, the control of carbon isotopes in the diamond crystal with an abrupt interface using isotopically purified CH_4 has recently been achieved [83,84]. However, besides the control of purity and crystalline quality, the challenges mostly rely on the stacking of layers with a precise amount of incorporated defects, nanoscale control, and extremely sharp interfaces in analogy with what has been achieved in the past with other semiconductors. This is not straightforward using the current PACVD technology and it is likely that these objectives in terms of material growth will be central to future applications.

Unintentional silicon-related defects originating from etching of the quartz reactor walls or viewports are also sometimes found. Silicon is rarely observed in natural diamond and its presence is often taken to be indicative of diamonds having a synthetic CVD origin [85]. A complex associating a silicon atom and a vacancy (Si–V centre) give rise to a zero phonon line at 737 nm (Fig. 9b) and 946 nm respectively for the negatively charged and neutral states [86], active in both absorption and luminescence. Just as for nitrogen there must exist a substitutional form of silicon in the diamond crystal. Although theoretically predicted [87], it has not yet been clearly observed experimentally. It is unclear at present whether Si–V would be a useful qubit for quantum information and more work is required to reach a better understanding of the structure and properties of this centre. For most applications though it should be avoided as it generates background luminescence. By choosing an appropriate shape and position for the dielectric windows and an efficient cooling to limit etching, its presence can be significantly reduced.

4.2. Extended defects

Impurities are sometimes found in an agglomerated form in CVD-grown diamond such as 3D graphite inclusions [88] or metal particles [89] at the substrate/film interface or embedded in the crystal which sometimes generate stress and dislocations. This emphasizes once more on the necessity to avoid any external contamination from the materials of the chamber together with proper growth conditions.

Dislocations are a type of extended defect that is found in CVD diamond films at concentrations in the range of 10^4 to 10^6 cm^{-2}. This is several orders of magnitude lower than natural diamonds but usually higher than the typical densities found in HPHT synthetic stones ($< 10^4$ cm^{-2}). The strong stress field that surrounds dislocations generates birefringence features visible as cross-shape patterns under cross-polarized filters (Fig. 10a) [90] which make them improper for optical applications requiring a high degree of homogeneity. Dislocations may generate deep levels in the bandgap resulting from dangling bonds along the dislocation line [91] which can behave as possible leakage paths and modify the electronic properties of the crystal. They are also efficient recombination centres for injected carriers. For example in the cathodoluminescence (CL) image of the free-exciton recombination intensity in Fig. 10b, dislocations are observed as dark lines due to efficient recombination at their core. In CL and photoluminescence (PL) dislocations are also usually responsible for a blue emission, visible in Fig. 10c.

To the contrary of natural diamond for which both screw and edge dislocations usually have lines lying along the ⟨110⟩ direction [92], CVD films grown on (001)-oriented substrates have threading dislocations propagating along the ⟨100⟩ growth direction [93]. Dislocations are mostly generated at the HPHT substrate/CVD layer interface due to the presence of stress, surface contamination, stacking faults or polishing damage [94]. By using an adapted surface treatment such as plasma etching [95,96], their density can be significantly decreased. Slicing thick crystals into plates along the growth direction is a way to overcome the detrimental effect of dislocations on the optical properties as the stress field now becomes perpendicular to the light path [22]. Alternating the growth direction by 90° has also been attempted by Gaukroger et al., showing that at least the dislocation propagation direction can be influenced by the growth direction [94]. By growing on substrates with angles from 20 to 40° relatively to the normal (100) surface dislocations can be successfully deviated as illustrated by the blue streaks in Fig. 10c.

Dislocations in CVD diamond have become a critical issue as the availability of good quality thick crystals is increasing. Exceptional type *IIa* HPHT substrates that can be reclaimed several times may help in achieving low dislocation density dia-

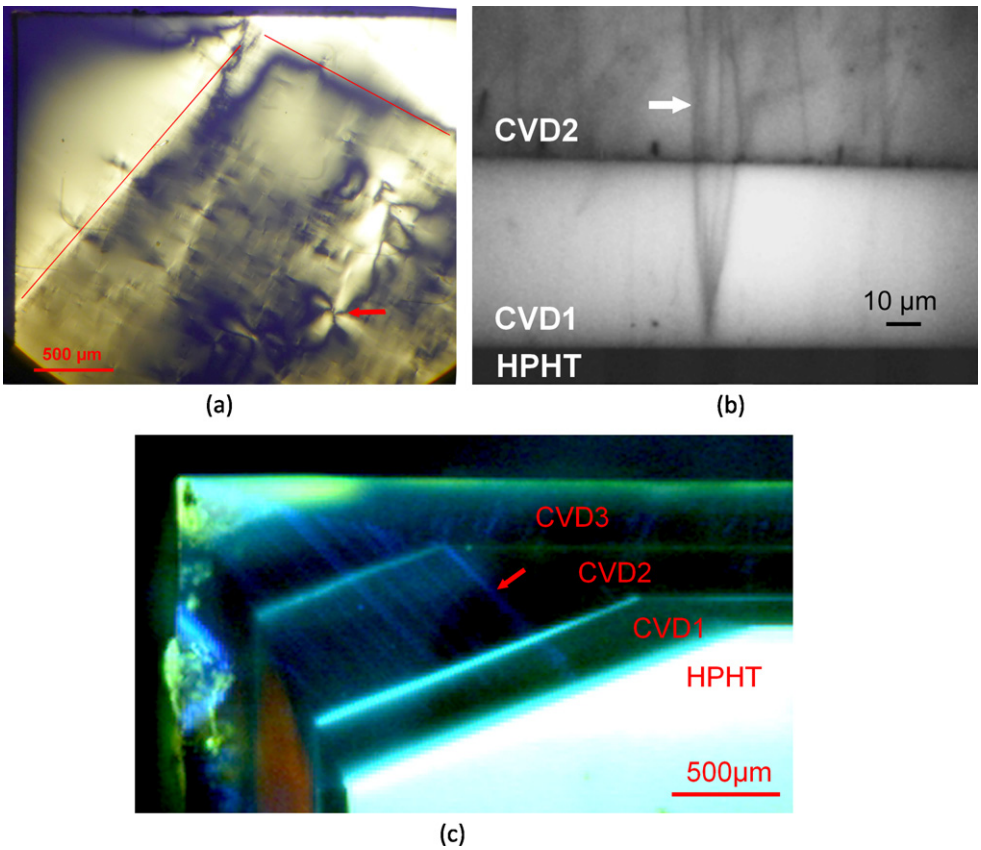

Fig. 10. (a) Birefringence image of the top surface of a freestanding CVD crystal; the red lines emphasize the initial position of the substrate and the arrow points at a large defect; (b) CL image at the free-exciton recombination wavelength (235 nm) of the cross-section of a CVD layer. It shows the nucleation of several dislocations at the HPHT/CVD1 interface and their propagation along the growth direction in successive CVD layers (Collab. J. Barjon, GEMaC, Université de Versailles–Saint-Quentin, CNRS); (c) PL image of the cross-section of a CVD layer grown on a 20° angled HPHT substrate; blue lines running perpendicular to the surface are related to dislocations (arrow); the thick lines parallel to the surface are indicative of growth interruptions.

Fig. 10. (a) Image de biréfringence de la surface d'un cristal CVD autosupporté ; les lignes rouges font apparaitre la position du substrat et la flèche pointe sur un défaut large ; (b) image CL à la longueur d'onde des excitons libres (235 nm) de la coupe d'un film CVD. La nucléation de dislocations à l'interface HPHT/CVD et la propagation le long de la direction de croissance et au travers de couches CVD successives (Collab. J. Barjon, GEMaC, Versailles–Saint-Quentin University, CNRS) ; (c) image PL de la coupe transversale d'un film CVD déposé sur un substrat présentant une désorientation de 20° ; les lignes bleues perpendiculaires à la surface proviennent de dislocations (flèche) ; les lignes épaisses parallèles à la surface indiquent les interruptions de croissance.

mond [97] but the development of dislocation reduction techniques will also be crucial in the next few years for exploiting the full potential of this material.

4.3. Doping with impurities

To be useful as a semiconductor for electronic applications, diamond's conductivity has to be modulated by introducing doping impurities into the crystal lattice. *n*-type doping has only been achieved using phosphorous, but it suffers from low incorporation efficiency in substitutional site, strong compensation and high activation energy (0.6 eV) [98]. Phosphorous doping has mostly been achieved on (111) orientations and only very rarely on conventional (100) substrates [99,100]. These difficulties have hindered the development of diamond devices based on *pn* junctions [101]. Despite intense research efforts in trying to improve the doping efficiency of phosphorous or finding other doping impurities [102], highly doped *n*-type diamond crystals cannot be easily obtained.

At LSPM we have focused our attention on *p*-type doping with a view to developing vertical unipolar power electronic devices such as Schottky diodes that are composed of a p^+/p^- stack sandwiched between an ohmic and a Schottky contact. *p*-type doping is easily obtained by adding boron during PACVD growth either through the use of diborane (B_2H_6) or trimethyl boron (TMB) [103]. Under specific growth conditions, doping efficiencies close to unity can be obtained [104]. Although the activation energy is relatively high (0.36 eV), it drops considerably as boron concentration gets to levels above 10^{19} cm^{-3} and down to metallic behaviour at about 3×10^{20} cm^{-3} [105]. Boron doped diamond films have been widely studied in a large range of concentrations either as active layers for electronics or as superconductors. However the reported films were usually no more than a few tens of micrometres thick especially for the high doping level thus limiting

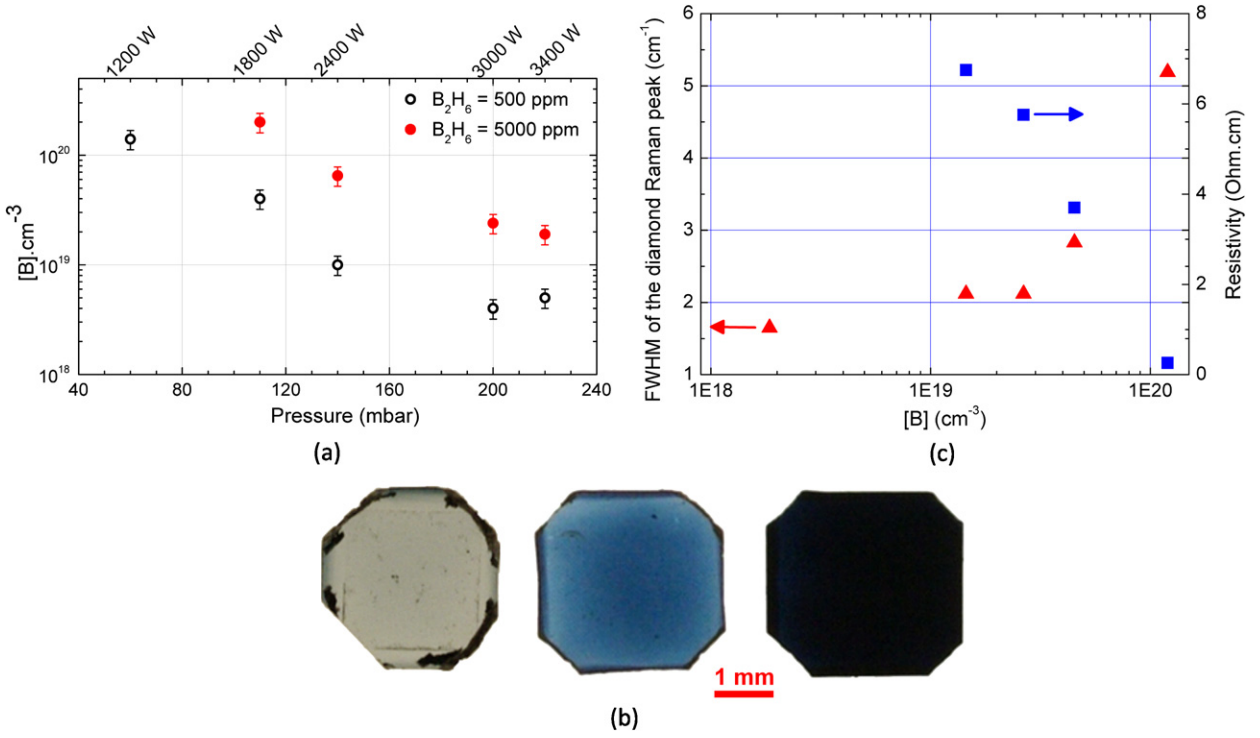

Fig. 11. (a) Evolution of boron doping as a function of different sets of MW power/pressure for different amounts of added boron in the gas phase; (b) freestanding boron diamond crystals having from left to right doping levels of 2×10^{18}, 2×10^{19} and 6×10^{19} cm^{-3}; (c) evolution of the crystalline quality evaluated by the width of the diamond Raman peak and of the resistivity as a function of doping level.

Fig. 11. (a) Évolution du dopage bore en fonction de différents couples puissance micro-onde / pression pour différentes quantités de bore ajouté dans la phase gazeuse ; (b) cristaux de diamant autosupportés avec des dopages de 2×10^{18}, 2×10^{19} et 6×10^{19} cm^{-3} ; (c) évolution de la qualité cristalline évaluée par la largeur du pic Raman et résistivité correspondante des films en fonction du dopage.

the operation to a pseudo-vertical geometry where all the contacts are made on the small top surface of the crystal. If high power electronic devices (> 3000 V, > 100 A) are to be fabricated, vertical configuration is much more favourable as it allows drawing larger currents, avoids current crowding at the contacts and makes use of the whole surface area of the synthetic crystals [106,16]. The main challenge relies on the ability to grow sufficiently thick highly boron-doped diamond crystals to be processed as freestanding plates and with a quality compatible to be used as a substrate for further growth of an active p^- layer.

To grow thick heavily doped diamond crystals, several issues have to be overcome. Under the high MWPD required to obtain good crystalline quality and high growth rates, the doping efficiency is very low, thus limiting the boron concentration to about 10^{19} cm^{-3} only. Moreover very high amounts of B_2H_6 have to be added to the discharge which promotes soot formation and prevents from running the reactor for an extensive period of time. Finally boron addition also leads to the formation of large {110} growth sectors at the edges of the crystal which induces stress up to a thickness after which the crystal breaks apart. It was found that the use of moderate MWPD is a good trade-off allowing thickening the layers while keeping reasonably high boron incorporation (Fig. 11a) [107]. Adding a small amount of oxygen (0.25%) during growth also helped limiting soot formation while inhibiting the formation of (110) sectors [58]. Unlike previous reports [108], under our conditions, oxygen did not significantly decrease boron incorporation. Using these optimized growth parameters, freestanding diamond plates (thickness > 200 µm) were successfully obtained with doping concentrations up to 10^{20} cm^{-3} showing a light blue to dark colouration depending on the doping level (Fig. 11b) [109]. These plates were found to exhibit high crystalline quality with a narrow diamond Raman peak that slightly enlarges as the doping level increases (Fig. 11c). Resistivity as low as 0.26 Ω cm for the highest doping level was measured opening the way to its use as a substrate for power electronic devices with unprecedented characteristics. Further work should be carried out to confirm doping homogeneity and measure the extended defect content in such crystals.

5. Summary

Over the last ten years the PACVD technique has gone through improvements and is now mature to produce high-quality high-purity single crystals with characteristics that outperform the best natural diamonds. It has provided the scientific community with an exceptional material that could allow developing new advanced applications. Nevertheless there remain many opened issues that need to be solved before this material can become widespread in industry.

In terms of dimensions, thicker crystals that can be easily sliced and processed are required. Obtaining diamond growth rates of a few tens of µm/h without adding impurities has proved possible by a joint increase of the power density and carbon content but it is significantly limited by the difficulty in keeping good crystal morphology all over the growth duration due to twinning at the edges and corners of the crystal. Obtaining millimetre-thick crystals requires complex processing steps and their synthesis is not so straightforward. As for the lateral dimensions of the crystal which constitutes one of the most relevant challenges for future applications in electronics, promising results have been obtained using mosaic assemblies of small crystals but further work is required to improve the interconnection between adjacent crystals and increase the total area.

The most common point defects in CVD diamond typically involve hydrogen, nitrogen, silicon and vacancies and have been widely studied. By using adapted growth conditions under a well-controlled environment it is possible to synthesize crystals having extremely low point defects and good isotopic purity that are relevant for applications such as quantum computing. Nevertheless reaching a nanoscale location of these defects and a perfect control of their structure and neighbouring atoms during growth is complicated using the current PACVD technique and will require more efforts. Nanoclusters, inclusions and most of all dislocations are also frequently found in CVD diamond and are becoming a serious issue as they plague the electronic characteristics of the crystal. Their occurrence can be significantly limited if selected exceptionally high-quality seeds that have gone through an appropriate surface treatment are used. Further improvement will require the development of strategies limiting threading dislocation propagation.

Finally some doping issues still remain unsolved. In particular, efficient *n*-type doping with low activation energy is mostly unavailable on conventional crystal orientations despite the strong efforts that have been devoted to improve it. The development of vertical power electronic devices will first rely on unipolar *p*-type boron-doped diamond. High-quality thick p^+ single crystals having a low conductivity recently obtained represent the first building block towards this goal if their defect content is reduced.

Acknowledgements

This work was supported by French DGE project DIAMONIX No. 08 2 90 6066 and French ANR project CROISADD No. ANR-11-ASTR-020.

References

[1] H. Kanda, in: P. Capper (Ed.), Bulk Crystal Growth in Electronic, Optical and Optoelectronic Materials, John Wiley and Sons, 2005.
[2] Y. Meng, M. Newville, S. Sutton, J. Rakovan, H.-K. Mao, Am. Mineral. 88 (2003) 1555.
[3] I. Kiflawi, H. Kanda, S.C. Lawson, Diam. Relat. Mater. 11 (2002) 204–211.
[4] R.C. Burns, A.I. Chumakov, S.H. Connell, D. Dube, H.P. Godfried, J.O. Hansen, J. Hartwig, J. Hoszowska, F. Masiello, L. Mkhonza, M. Rebak, A. Rommevaux, R. Setshedi, P.V. Vaerenbergh, J. Phys. Condens. Matter 21 (2009) 364224.
[5] W.Q. Liu, H.A. Ma, X.L. Li, Z.Z. Liang, R. Li, X. Jia, Diam. Relat. Mater. 16 (2007) 1486–1489.
[6] A. Tallaire, J. Achard, F. Silva, R.S. Sussmann, A. Gicquel, Diam. Relat. Mater. 14 (2005) 249–254.
[7] T. Bauer, M. Schreck, H. Sternschulte, B. Stritzker, Diam. Relat. Mater. 14 (2005) 266–271.
[8] C.-s. Yan, Y.K. Vohra, H.-k. Mao, R.J. Hemley, Proc. Natl. Acad. Sci. USA 99 (2002) 12523–12525.
[9] G. Bogdan, M. Nesládek, J. D'Haen, J. Maes, V.V. Moshchalkov, K. Haenen, M. D'Olieslaeger, Phys. Status Solidi, a Appl. Res. 202 (2005) 2066–2072.
[10] T. Teraji, Phys. Status Solidi, a Appl. Res. 203 (2006) 3324–3357.
[11] P.M. Martineau, S.C. Lawson, A.J. Taylor, S.J. Quinn, D.J.F. Evans, M.J. Crowder, Gems. Gemol. 40 (2004) 2.
[12] W.Y. Wang, T. Moses, R.C. Linares, J.E. Shigley, M. Hall, J.E. Butler, Gems. Gemol. 39 (2003) 268–283.
[13] J. Achard, A. Tallaire, R. Sussmann, F. Silva, A. Gicquel, J. Cryst. Growth 284 (2005) 396–405.
[14] R.S. Balmer, J.R. Brandon, S.L. Clewes, H.K. Dhillon, J.M. Dodson, I. Friel, P.N. Inglis, T.D. Madgwick, M.L. Markham, T.P. Mollart, N. Perkins, G.A. Scarsbrook, D.J. Twitchen, A.J. Whitehead, J.J. Wilman, S.M. Woollard, J. Phys. Condens. Matter 21 (2009) 364221.
[15] P.N. Volpe, J. Pernot, P. Muret, F. Omnes, Appl. Phys. Lett. 94 (2009) 092102–092103.
[16] J. Achard, F. Silva, R. Issaoui, O. Brinza, A. Tallaire, H. Schneider, K. Isoird, H. Ding, S. Koné, M.A. Pinault, F. Jomard, A. Gicquel, Diam. Relat. Mater. 20 (2011) 145–152.
[17] D. Francis, F. Faili, D. Babic, F. Ejeckam, A. Nurmikko, H. Maris, Diam. Relat. Mater. 19 (2010) 229–233.
[18] M. Dipalo, Z. Gao, J. Scharpf, C. Pietzka, M. Alomari, F. Medjdoub, J.F. Carlin, N. Grandjean, S. Delage, E. Kohn, Diam. Relat. Mater. 18 (2009) 884–889.
[19] M.L. Markham, J.M. Dodson, G.A. Scarsbrook, D.J. Twitchen, G. Balasubramanian, F. Jelezko, J. Wrachtrup, Diam. Relat. Mater. 20 (2011) 134–139.
[20] G. Balasubramanian, P. Neumann, D. Twitchen, M. Markham, R. Kolesov, N. Mizuochi, J. Isoya, J. Achard, J. Beck, J. Tissler, V. Jacques, P.R. Hemmer, F. Jelezko, J. Wrachtrup, Nat. Mater. 8 (2009) 383–387.
[21] W. Lubeigt, G.M. Bonner, J.E. Hastie, M.D. Dawson, D. Burns, A.J. Kemp, Opt. Express 18 (2010) 16765–16770.
[22] I. Friel, S.L. Clewes, H.K. Dhillon, N. Perkins, D.J. Twitchen, G.A. Scarsbrook, Diam. Relat. Mater. 18 (2009) 808–815.
[23] N. Tranchant, D. Tromson, C. Descamps, A. Isambert, H. Hamrita, P. Bergonzo, M. Nesladek, Diam. Relat. Mater. 17 (2008) 1297–1301.
[24] J.F. Hochedez, P. Bergonzo, M.C. Castex, P. Dhez, O. Hainaut, M. Sacchi, J. Alvarez, H. Boyer, A. Deneuville, P. Gibart, B. Guizard, J.P. Kleider, P. Lemaire, C. Mer, E. Monroy, E. Munoz, P. Muret, F. Omnes, J.L. Pau, V. Ralchenko, D. Tromson, E. Verwichte, J.C. Vial, Diam. Relat. Mater. 10 (2001) 673–680.
[25] S.J. Harris, Appl. Phys. Lett. 56 (1990) 2298–2300.
[26] A. Gicquel, N. Derkaoui, C. Rond, F. Benedic, G. Cicala, D. Moneger, K. Hassouni, Chem. Phys. 398 (2012) 239–247.
[27] A. Gicquel, F. Silva, K. Hassouni, J. Electrochem. Soc. 147 (2000) 2218–2226.
[28] A. Gicquel, K. Hassouni, F. Silva, J. Achard, Curr. Appl. Phys. 1 (2001) 479–496.
[29] K. Hassouni, F. Silva, A. Gicquel, J. Phys. D, Appl. Phys. 43 (2010) 153001.
[30] J. Ma, J.C. Richley, D.R.W. Davies, M.N.R. Ashfold, Y.A. Mankelevich, J. Phys. Chem. A, Mol. Spectrosc. Kinet. Environ. Gen. Theory 114 (2010) 10076–10089.
[31] T. Teraji, T. Ito, J. Cryst. Growth 271 (2004) 409–419.
[32] F. Silva, K. Hassouni, X. Bonnin, A. Gicquel, J. Phys. Condens. Matter 21 (2009) 364202.

[33] Y. Gu, J. Lu, T. Grotjohn, T. Schuelke, J. Asmussen, Diam. Relat. Mater. 24 (2012) 210–214.
[34] X.J. Li, W.Z. Tang, S.W. Yu, S.K. Zhang, G.C. Chen, F.X. Lu, Diam. Relat. Mater. 20 (2011) 480–484.
[35] M. Fischer, S. Gsell, M. Schreck, R. Brescia, B. Stritzker, Diam. Relat. Mater. 17 (2008) 1035–1038.
[36] S. Washiyama, S. Mita, K. Suzuki, A. Sawabe, Appl. Phys. Express 4 (2011).
[37] J.E. Butler, I. Oleynik, Philos. Trans. R. Soc., Math. Phys. Eng. Sci. 366 (2008) 295–311.
[38] J. Asmussen, T.A. Grotjohn, T. Schuelke, M.F. Becker, M.K. Yaran, D.J. King, S. Wicklein, D.K. Reinhard, Appl. Phys. Lett. 93 (2008) 031502–031503.
[39] J.E. Butler, R.L. Woodin, Philos. Trans. R. Soc., Math. Phys. Eng. Sci. 342 (1993) 209–224.
[40] H. Maeda, K. Ohtsubo, M. Kameta, T. Saito, K. Kusakabe, S. Morooka, T. Asano, Diam. Relat. Mater. 7 (1998) 88–95.
[41] C.C. Battaile, D.J. Srolovitz, I.I. Oleinik, D.G. Pettifor, A.P. Sutton, S.J. Harris, J.E. Butler, J. Chem. Phys. 111 (1999) 4291–4299.
[42] C. Wild, R. Kohl, N. Herres, W. Muller-Sebert, P. Koidl, Diam. Relat. Mater. 3 (1994) 373–381.
[43] A. Chayahara, Y. Mokuno, Y. Horino, Y. Takasu, H. Kato, H. Yoshikawa, N. Fujimori, Diam. Relat. Mater. 13 (2004) 1954–1958.
[44] J. Achard, F. Silva, O. Brinza, A. Tallaire, A. Gicquel, Diam. Relat. Mater. 16 (2007) 685–689.
[45] T. Frauenheim, G. Jungnickel, P. Sitch, M. Kaukonen, F. Weich, J. Widany, D. Porezag, Diam. Relat. Mater. 7 (1998) 348–355.
[46] S. Dunst, H. Sternschulte, M. Schreck, Appl. Phys. Lett. 94 (2009) 224101–224103.
[47] I. Markov, Crystal Growth for Beginners, Fundamentals of Nucleation, Growth and Epitaxy, World Scientific, 2004.
[48] M. Ogura, H. Kato, T. Makino, H. Okushi, S. Yamasaki, J. Cryst. Growth 317 (2011) 60–63.
[49] J. Achard, F. Silva, A. Tallaire, X. Bonnin, G. Lombardi, K. Hassouni, A. Gicquel, J. Phys. D, Appl. Phys. 40 (2007) 6175–6188.
[50] X. Duten, A. Rousseau, A. Gicquel, K. Hassouni, P. Leprince, J. Phys. D, Appl. Phys. 35 (2002) 1939–1945.
[51] A. Gicquel, F. Silva, X. Duten, K. Hassouni, G. Lombardi, A. Rousseau, French Patent, July 2004, FR2849867.
[52] A. Gicquel, F. Silva, X. Duten, K. Hassouni, G. Lombardi, A. Rousseau, U.S. Patent, February 2010, 7662441 B2.
[53] O.J.L. Fox, J. Ma, P.W. May, M.N.R. Ashfold, Y.A. Mankelevich, Diam. Relat. Mater. 18 (2009) 750–758.
[54] D. Moneger, F. Benedic, R. Azouani, F. Chelibane, O. Syll, F. Silva, A. Gicquel, Diam. Relat. Mater. 16 (2007) 1295–1299.
[55] A. Tallaire, C. Rond, F. Bénédic, O. Brinza, J. Achard, F. Silva, A. Gicquel, Phys. Status Solidi, a Appl. Res. 208 (2011) 2028–2032.
[56] Y.-S. Han, Y.-K. Kim, J.-Y. Lee, Thin Solid Films 310 (1997) 39–46.
[57] H. Okushi, H. Watanabe, S. Ri, S. Yamanaka, D. Takeuchi, J. Cryst. Growth 237–239 (2002) 1269–1276.
[58] R. Issaoui, J. Achard, F. Silva, A. Tallaire, V. Mille, A. Gicquel, Phys. Status Solidi, a Appl. Res. 208 (2011) 2023–2027.
[59] F. Silva, J. Achard, X. Bonnin, A. Michau, A. Tallaire, O. Brinza, A. Gicquel, Phys. Status Solidi, a Appl. Res. 203 (2006) 3049–3055.
[60] C. Wild, P. Koild, W. Müller-Sebert, H. Walcher, R. Kohl, N. Herres, R. Locher, R. Samlenski, R. Brenn, Diam. Relat. Mater. 2 (1993) 158.
[61] F. Silva, J. Achard, X. Bonnin, O. Brinza, A. Michau, A. Secroun, K. De Corte, S. Felton, M. Newton, A. Gicquel, Diam. Relat. Mater. 17 (2008) 1067–1075.
[62] O. Brinza, J. Achard, F. Silva, X. Bonnin, P. Barroy, K. De Corte, A. Gicquel, Phys. Status Solidi, a Appl. Res. 205 (2008) 2114–2120.
[63] A. Tallaire, J. Barjon, O. Brinza, J. Achard, F. Silva, V. Mille, R. Issaoui, A. Tardieu, A. Gicquel, Diam. Relat. Mater. 20 (2011) 875–881.
[64] F. Silva, J. Achard, O. Brinza, X. Bonnin, K. Hassouni, A. Anthonis, K. De Corte, J. Barjon, Diam. Relat. Mater. 18 (2009) 682–697.
[65] Y. Mokuno, A. Chayahara, Y. Soda, Y. Horino, N. Fujimori, Diam. Relat. Mater. 14 (2005) 1743–1746.
[66] M.W. Geis, N.N. Efremow, R. Susalka, J.C. Twichell, K.A. Snail, C. Spiro, B. Sweeting, S. Holly, Diam. Relat. Mater. 4 (1994) 76–82.
[67] C. Findeling-Dufour, A. Gicquel, Thin Solid Films 308–309 (1997) 178–185.
[68] G. Janssen, L.J. Giling, Diam. Relat. Mater. 4 (1995) 1025–1031.
[69] H. Yamada, A. Chayahara, Y. Mokuno, H. Umezawa, S.-i. Shikata, N. Fujimori, Appl. Phys. Express 3 (2010) 051301.
[70] H. Yamada, A. Chayahara, H. Umezawa, N. Tsubouchi, Y. Mokuno, S. Shikata, Diam. Relat. Mater. 24 (2012) 29–33.
[71] A.M. Zaïtsev, Optical Properties of Diamond: A Data Handbook, Springer, 2001.
[72] J.M. Maki, F. Tuomisto, C.J. Kelly, D. Fisher, P.M. Martineau, J. Phys. Condens. Matter 21 (2009) 364216.
[73] I. Kiflawi, D. Fisher, H. Kanda, G. Sittas, Diam. Relat. Mater. 5 (1996) 1516–1518.
[74] C. Glover, M.E. Newton, P.M. Martineau, S. Quinn, D.J. Twitchen, Phys. Rev. Lett. 92 (2004) 135502.
[75] J. Chevallier, A. Lusson, D. Ballutaud, B. Theys, F. Jomard, A. Deneuville, M. Bernard, E. Gheeraert, E. Bustarret, Diam. Relat. Mater. 10 (2001) 399–404.
[76] A. Stacey, T.J. Karle, L.P. McGuinness, B.C. Gibson, K. Ganesan, S. Tomljenovic-Hanic, A.D. Greentree, A. Hoffman, R.G. Beausoleil, S. Prawer, Appl. Phys. Lett. 100 (2012) 071902.
[77] S.J. Charles, J.E. Butler, B.N. Feygelson, M.E. Newton, D.L. Carroll, J.W. Steeds, H. Darwish, C.S. Yan, H.K. Mao, R.J. Hemley, Phys. Status Solidi, a Appl. Res. 201 (2004) 2473–2485.
[78] A. Tallaire, A.T. Collins, D. Charles, J. Achard, R. Sussmann, A. Gicquel, M.E. Newton, A.M. Edmonds, R.J. Cruddace, Diam. Relat. Mater. 15 (2006) 1700–1707.
[79] J. Meijer, B. Burchard, M. Domhan, C. Wittmann, T. Gaebel, I. Popa, F. Jelezko, J. Wrachtrup, Appl. Phys. Lett. 87 (2005) 261909.
[80] P. Spinicelli, A. Dréau, L.R.F. Silva, J. Achard, S. Xavier, S. Bansropun, T. Debuisschert, S. Pezzagna, J. Meijer, V. Jacques, J.-F. Roch, New J. Phys. 13 (2011) 025014.
[81] S. Pezzagna, D. Wildanger, P. Mazarov, A.D. Wieck, Y. Sarov, I. Rangelow, B. Naydenov, F. Jelezko, S.W. Hell, J. Meijer, Small 6 (2010) 2117–2121.
[82] V. Petráková, M. Nesládek, A. Taylor, F. Fendrych, P. Cígler, M. Ledvina, J. Vacík, J. Štursa, J. Kučka, Phys. Status Solidi, a Appl. Res. 208 (2011) 2051–2056.
[83] J. Barjon, F. Jomard, A. Tallaire, J. Achard, F. Silva, Appl. Phys. Lett. 100 (2012) 122107.
[84] H. Watanabe, C.E. Nebel, S. Shikata, Science 324 (2009) 1425–1428.
[85] B. Willems, A. Tallaire, J. Barjon, Gems. Gemol. 47 (2011) 202–207.
[86] A.M. Edmonds, M.E. Newton, P.M. Martineau, D.J. Twitchen, S.D. Williams, Phys. Rev. B 77 (2008) 245205.
[87] J.P. Goss, P.R. Briddon, M.J. Rayson, S.J. Sque, R. Jones, Phys. Rev. B 72 (2005) 035214.
[88] A. Crisci, F. Baillet, M. Mermoux, G. Bogdan, M. Nesládek, K. Haenen, Phys. Status Solidi, a Appl. Res. 208 (2011) 2038–2044.
[89] A. Tallaire, M. Kasu, K. Ueda, T. Makimoto, Diam. Relat. Mater. 17 (2008) 60–65.
[90] A. Secroun, O. Brinza, A. Tardieu, J. Achard, F. Silva, X. Bonnin, K. De Corte, A. Anthonis, M.E. Newton, J. Ristein, P. Geithner, A. Gicquel, Phys. Status Solidi, a Appl. Res. 204 (2007) 4298–4304.
[91] C.J. Fall, A.T. Blumenau, R. Jones, P.R. Briddon, T. Frauenheim, A. Gutierrez-Sosa, U. Bangert, A.E. Mora, J.W. Steeds, J.E. Butler, Phys. Rev. B 65 (2002) 205206.
[92] A.T. Blumenau, M.I. Heggie, C.J. Fall, R. Jones, T. Frauenheim, Phys. Rev. B 65 (2002) 205205.
[93] N. Fujita, A.T. Blumenau, R. Jones, S. Öberg, P.R. Briddon, Phys. Status Solidi, a Appl. Res. 203 (2006) 3070–3075.
[94] M.P. Gaukroger, P.M. Martineau, M.J. Crowder, I. Friel, S.D. Williams, D.J. Twitchen, Diam. Relat. Mater. 17 (2008) 262–269.
[95] A. Tallaire, J. Achard, F. Silva, R.S. Sussmann, A. Gicquel, E. Rzepka, Phys. Status Solidi, a Appl. Res. 201 (2004) 2419–2424.
[96] P.-N. Volpe, P. Muret, F. Omnes, J. Achard, F. Silva, O. Brinza, A. Gicquel, Diam. Relat. Mater. 18 (2009) 1205–1210.
[97] J.H. Kaneko, F. Fujita, Y. Konno, T. Gotoh, N. Nishi, H. Watanabe, A. Chayahara, H. Umezawa, N. Tsubouchi, S. Shikata, M. Isobe, Diam. Relat. Mater. 26 (2012) 45–49.
[98] S. Koizumi, M. Suzuki, Phys. Status Solidi, a Appl. Res. 203 (2006) 3358–3366.

[99] H. Kato, H. Watanabe, S. Yamasaki, H. Okushi, Diam. Relat. Mater. 15 (2006) 548–553.
[100] M.A. Pinault-Thaury, B. Berini, I. Stenger, E. Chikoidze, A. Lusson, F. Jomard, J. Chevallier, J. Barjon, Appl. Phys. Lett. 100 (2012) 192104–192109.
[101] S. Koizumi, K. Watanabe, M. Hasegawa, H. Kanda, Diam. Relat. Mater. 11 (2002) 307–311.
[102] G. Frangieh, M.A. Pinault, J. Barjon, F. Jomard, J. Chevallier, Phys. Status Solidi, a Appl. Res. 205 (2008) 2207–2210.
[103] A. Deneuville, Semicond. Semimet. 76 (2003) 183–238.
[104] R. Ramamurti, M. Becker, T. Schuelke, T. Grotjohn, D. Reinhard, J. Asmussen, Diam. Relat. Mater. 17 (2008) 1320–1323.
[105] J.P. Lagrange, A. Deneuville, E. Gheeraert, Diam. Relat. Mater. 7 (1998) 1390–1393.
[106] H. Umezawa, K. Ikeda, N. Tatsumi, K. Ramanujam, S.-i. Shikata, Diam. Relat. Mater. 18 (2009) 1196–1199.
[107] R. Issaoui, J. Achard, F. Silva, A. Tallaire, A. Tardieu, A. Gicquel, M.A. Pinault, F. Jomard, Appl. Phys. Lett. 97 (2010) 182101.
[108] F. Omnès, P. Muret, P.-N. Volpe, M. Wade, J. Pernot, F. Jomard, Diam. Relat. Mater. 20 (2011) 912–916.
[109] R. Issaoui, J. Achard, A. Tallaire, F. Silva, A. Gicquel, R. Bisaro, B. Servet, G. Garry, J. Barjon, AIP 100 (2012) 122109.